Electronic Supplementary Material (ESI) for Catalysis Science & Technology.

Supporting Information for

Stability of the Ketyl Radical as a Descriptor in the Electrochemical Coupling of Benzaldehyde

Jacob Anibal, Arnav Malkani and Bingjun Xu*

Center for Catalytic Science and Technology, Department of Chemical and Biomolecular Engineering, University of Delaware, 150 Academy Street, Newark DE, 19716

*bxu@udel.edu

Experimental

Electrochemical Reactivity Tests

Electrochemical activity tests were performed in an H-cell using a three-electrode configuration. The electrolyte consisted of 0.5 M phosphate buffer at pH 4.6. For benzaldehyde reduction experiments, benzaldehyde was added to the buffer to achieve a 20 mM concentration. All experiments occurred in a closed cell, with a balloon used to collect product gases and maintain isobaric conditions (Figures S1A and S1B). Metal foils of Pt, Pd, Au, and Cu served as the working electrodes, with a Ag/AgCl reference electrode (3 M, BASi). Subsequently, potentials were converted to the RHE scale and all reported potentials in this work correspond this scale. Prior to testing, the foils were cleaned by three sequential etches in aqua regia (75% HCl, 25% HNO_3) and piranha etch (75% H_2O_2 (30%), 25% HSO_4). A graphite rod served as the counter electrode, with a Nafion 211 membrane separating the anode and cathode compartments. Activity tests were performed potentiostatically, with potential controlled using either a VersaStat3 (Princeton Applied Research) or Solartron SI 1287 potentiostat (Ametek). Results did not vary significantly between potentiostats. Solution resistance was measured before each test, with uncompensated resistance typically below six ohms. To avoid known benzaldehyde mass transport limitations[1], all tests were stirred with a stir bar at a rate of ~800 rpm. To further ensure a lack of mass transport, control tests were also performed with ~300 rpm for Cu and Pd at -0.5 V. Both tests show comparable rates to those obtained with 800 rpm. A typical activity test occurred in five steps. First, the electrolyte was purged with Ar for 30 min to remove dissolved oxygen. The working electrode was then pre-reduced at -0.2 V for 30 min to remove surface oxides. An hour long HER control was then performed in pure phosphate buffer. This control occurred at the same potential as the subsequent benzaldehyde reduction and served as a check on cell leak tightness. Benzaldehyde was then mixed into solution at open circuit for 30 min, followed by the hour-long benzaldehyde reduction reactivity test at either -0.2 or -0.5 V. Ar was purged between each electrochemical reduction step to remove residual gases from the head space.

Product Identification and Quantification

The main products of benzyl alcohol and hydrobenzoin were identified by gas chromatography (GC) and proton nuclear magnetic resonance (NMR) by comparison to purchased pure standards. GC-MS data was also collected to confirm these assignments and check for any trace side products. Benzyl alcohol was quantified by GC following an extraction with ethyl acetate. Ethyl acetate was added to the product solution in a 2:1 volume ratio and vortexed for one minute to ensure good mixing. The aqueous phase was then removed, and the benzyl alcohol in the organic phase quantified using a calibrated GC. Control tests showed extraction efficiencies of > 95%. Hydrobenzoin was quantified using NMR. NMR spectra were collected for the aqueous reduction product using an AV600 NMR spectrometer (Bruker) with 64 co-averaged scans. The built-in water suppression program was used to remove background water interference. The NMR spectra show peaks for both the dl and meso hydrobenzoin. Unfortunately, the meso hydrobenzoin NMR peaks overlap with those of benzyl alcohol. To account for this overlap, the benzyl alcohol quantified by GC was converted to an NMR area (via calibration curve) and subtracted from the

meso hydrobenzoin area. Hydrogen production was quantified by GC. Hydrogen volume was determined by GC peak area and converted to molar production using the combined balloon and headspace volume. The rates for all products were area normalized using geometric surface area.

In Situ ATR-SEIRAS Measurements

In Situ ATR-SEIRAS spectra were collected using a custom spectroscopic cell with side mounted ATR crystal to allow for stirring. The cell has been described in detail previously.[2] Briefly, the cell consisted of a glass and Teflon anode compartment separated from a glass anode compartment by a Nafion 211 membrane. A graphite rod and Ag/AgCl served as the counter and reference electrode, respectively. The working electrode consisted of a thin metal film deposited onto a 3.14 cm^2 Si ATR-crystal (2 cm diameter), with a strip of copper tape providing an external electrical connection to the potentiostat. A Teflon wrapped O-ring served as the seal between the crystal and cell and covered the Cu tape. The Au and Cu films were chemically deposited using methods described previously.[3–5] These Au and Cu films consist of poly crystalline islands ~50 nm in size.[3–5] Pt and Pd films were electroplated onto Au films by multiple galvanostatic depositions based on the method of Yan et al.[6] Pt films were plated using three, 180 s depositions at -800 µA with a Pt counter electrode. Pd was plated using four, 160 s depositions at -40 µA with a Pd counter electrode. The additional depositions were required as the original procedure of Yan resulted in very thin films. The electroplating procedure results in a slightly different morphology, with smaller Pt and Pd particles deposited on top of the underlying Au islands.[6] All films were activated by cyclic voltammetry before use. Post activation, a spectrum was collected for atmospheric water vapor subtraction. Good atmospheric water subtraction was essential, as benzaldehyde showed many bands on the order of atmospheric water fluctuation. Subtraction spectra were collected at open circuit, except for Cu, which was collected at 0 V to avoid film dissolution. All spectra reported in this work have had atmospheric water subtracted. The ATR-SIERAS spectra were collected using a Carry 660 infrared spectrometer (Agilent Technologies) with a liquid nitrogen cooled MCT detector. Spectra were collected at 4 cm^{-1} resolution, with 64 and 128 co-added scans for the spectra and background, respectively. Backgrounds were collected at -0.2 V for all metals except Pt, which was collected at 0 V. The higher background potential was required due to film instability caused by hydrogen bubble formation. Pt films remained stable only above -0.2 V. Potential was controlled using a Solartron SI 1287 potentiostat. Ohmic resistance was measured before testing using impedance and actively compensated (using potentiostat settings) to give an effective resistance of six ohms or less. Ar was bubbled through solution prior to testing to remove dissolved oxygen. Stirring was provided by a stir bar at ~ 800 rpm.

Given the known sensitivity of ATR-SEIRAS to contamination,[7] special care was required in conducting the ATR-SEIRAS experiments. Au and Cu films showed great spectroscopic sensitivity to trace metal impurities. To avoid these contaminants, the spectroscopic cell was soaked twice in DI water with excess iminodiacetate resin (Chelex 100, Sigma Aldrich). The buffer solution was also treated with Chelex to remove trace metal impurities. Care was also required for Pt and Pd, but for a different issue. These films showed sensitivity to contamination by trace organic contaminants and dissolved CO_2. Both resulted in contaminant CO peaks at reducing conditions in pure buffer, although the peaks were much smaller than those formed by adding benzaldehyde. Mitigating this CO contamination required extensive pre-test procedures. Before

testing, the spectroscopic cell was cleaned with Piranha etch, then rinsed and twice boiled in DI water. The phosphate buffer was also purged with Ar over night to remove any dissolved CO_2 or volatile organic species.

Reagents and Others

Benzaldehyde (98%), benzyl alcohol (98%), and hydrobenzoin (98%, non-stereo specific) were all obtained from Sigma-Aldrich and used as received. Meso-hydrobenzoin (98%) was obtained from TCI America and also used as received. Phosphate buffer was made from NaH_2PO_4 (Certified ACS, Fisher) and double dionized, distilled (DI) water (Barnstead Mega Pure Water Purification System). The same DI water was used for rinsing, soaking, and cleaning. Buffer pH was checked using a pH meter (Okion) and adjusted to 4.6 by adding a small amount of Na_2HPO_4 (>99%, Sigma-Aldrich). Ar (99.999%) and CO (99.999%) gases were obtained from Matheson. Aqua regia was made from a 3:1 mixture of HCl (Fisher) and HNO_3 (Fisher). Piranha etch consisted of a 3:1 mixture of H_2SO_4 (Fisher) and 30% H_2O_2 (Sigma-Aldrich).

Nafion 211 membranes were obtained from the Fuel Cell Store. Prior to use, the membranes were treated with 5% H_2O_2 at 60 ºC for one hour, followed by twice soaking in DI water. Treated membranes were then stored in DI water. Graphite rods were obtained from the Graphite Store and sonicated prior to use to remove loose carbon. Balloons were constructed from a latex glove finger and 20 mL syringe and sealed with epoxy (JB Weld) (Figure S1C). Working electrodes were made from Au (99.99%, Alfa-Aesar), Cu (99.998%, Sigma-Aldrich), Pt (99.99%, Alfa-Aesar), and Pd (99.9%, Alfa-Aeasr) foils. Foil strips were connected to Ni wire using Cu tape to form electrodes. The Ni-Cu junction was then wrapped in Teflon tape and remained above the electrolyte level to avoid Cu contamination. Before use, the electrodes were cleaned by three successive, five second etches in aqua regia and piranha solution.

References

1. Y. Song, U. Sanyal, D. Pangotra, J. D. Holladay, D. M. Camaioni, O. Y. Gutiérrez and J. A. Lercher, *J. Catal.*, 2018, **359**, 68–75.
2. M. Dunwell, X. Yang, B. P. Setzler, J. Anibal, Y. Yan and B. Xu, *ACS Catal.*, 2018, **8**, 3999–4008.
3. H. Miyake, S. Ye and M. Osawa, *Electrochem. commun.*, 2002, **4**, 973–977.
4. M. Dunwell, Y. Yan and B. Xu, *Surf. Sci.*, 2015, **650**, 51–56.
5. A. S. Malkani, M. Dunwell and B. Xu, *ACS Catal.*, 2019, **9**, 474–478.
6. Y. G. Yan, Q. X. Li, S. J. Huo, M. Ma, W. Bin Cai and M. Osawa, *J. Phys. Chem. B*, 2005, **109**, 7900–7906.
7. M. Dunwell, X. Yang, Y. Yan and B. Xu, *J. Phys. Chem. C*, 2018, **122**, 24658–24664.

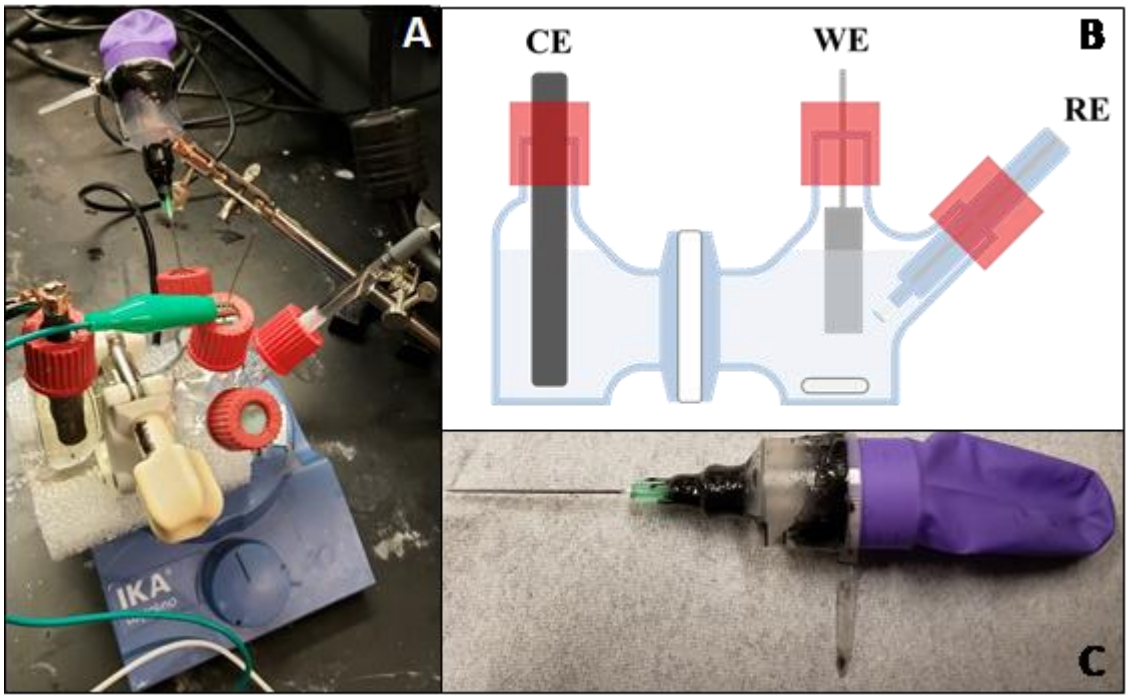

Figure S1. (A) Photograph of the electrochemical cell in operation. **(B)** Schematic of the electrochemical reduction cell. **(C)** Photograph of the constructed balloon.

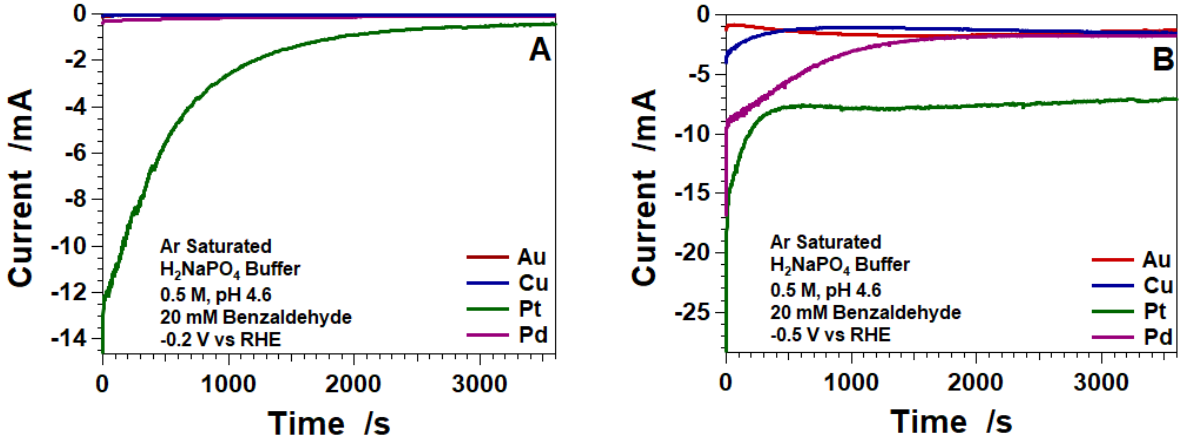

Figure S2. (A) Representative current profiles for benzaldehyde reduction at -0.2 V. **(B)** The same as (A), but -0.5 V. All reactivity tests were performed with an 800 rpm stir rate.

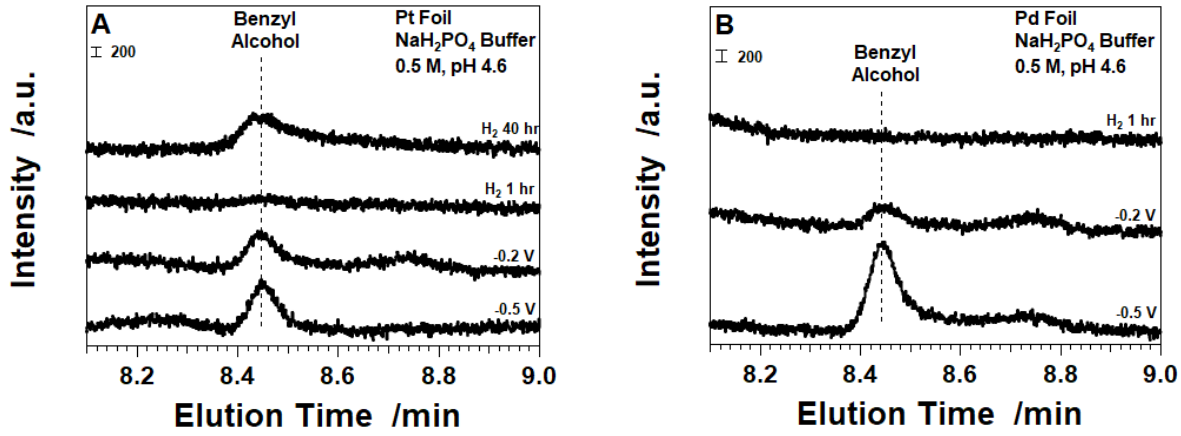

Figure S3. GC chromatogram comparing benzaldehyde reduction by hydrogen gas on **(A)** Pt and **(B)** Pd (top traces) to electrochemical reduction (bottom traces). All reductions were performed at room temperature, with the electrochemical tests in Ar purged buffer solution.

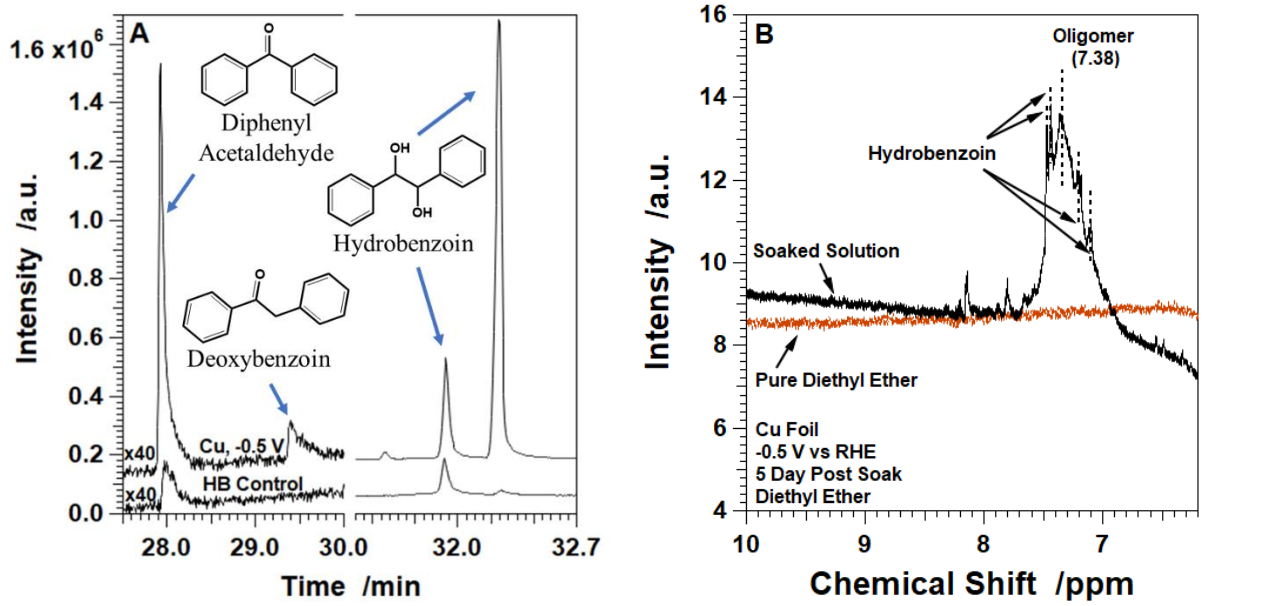

Figure S4. (A) GC chromatographs for the Cu dimer reduction products at -0.5 V (alcohol not shown) and a control sample of 1 mM benzaldehyde after 3 months storage at room temperature. **(B)** NMR spectra collected for diethyl ether solution after soaking the Cu electrode. The Cu electrode was soaked for five days after a 1hour benzaldehyde reduction test at -0.5 V.

Table S1. Summary of Infrared Peak Assignments

Peak Position /cm^{-1}	Peak Assignment	Stark Rate cm^{-1}/V	Surfaces Present	Figures Present
1699	C=O Stretch, Bulk Benz[1]	NA	Si	S5
1596	ν_{8a} Ring Mode, Bulk Benz[1]	NA	Si	S5
1584	ν_{8b} Ring Mode, Bulk Benz[1]	NA	Si	S5
1454	ν_{18b} Ring Mode, Bulk Benz[1]	NA	Si	S5
1390	CH Aldehyde. Bend, Bulk Benz[1]	NA	Si	S5
1310	ν_3 Ring Mode, Bulk Benz[1]	NA	Si	S5
1496	Bulk Benz Alc., likely ν_{18a} Ring Mode[1,2]	NA	Si	S5
1453	Bulk Benz Alc., likely ν_{18b} Ring Mode[1,2]	NA	Si	S5
1650-1630	δ(OH) Mode, Bulk/Adsorbed Water	NA[a]	Au, Cu, Pt, Pd	3, 4, 5A, 6, 7A, S6-S9, S11
~1700 (sh)[b]	C=O Stretch, Bulk Benz[1]	0	Au, Cu	2A, 3A, S6, 3A
~1694[b]	C=O Stretch, Adsorbed Benz[3]	0	Au, Cu, Pt, Pd	2A, 3A, 4B, 5A, 6B, 7A, S6-S8, S11
1598[c]	ν_{8a} Ring Mode, Benz[1,c]	0	Au, Cu	2A, S6-S8
1584[c]	ν_{8b} Ring Mode, Benz[1,c]	0	Au, Cu	2A, S6-S8
1455[c]	ν_{18b} Ring Mode, Benz[1,c]	0	Au, Cu	2A, S6
1310[c]	ν_3 Ring Mode, Benz[1,c]	0	Au, Cu	2A, S6-S7
1492	Benzoic Acid (contaminant), Adsorbed[2]	0	Au	2A, 2B
1366-1388	Benzoate, Adsorbed	24	Au, Pt	2C, S11B
2921	Benz Alc., Ring H Stretch[1,2]	0	Cu	3C, S10B
2851	Benz Alc., Ring H Stretch[1,2]	0	Cu	3C, S10B
1496[d]	Benz Alc., likely ν_{18a} Ring Mode[1,2]	0	Au, Cu[e]	2A, 3B, S6
1453[d]	Benz Alc., likely ν_{18b} Ring Mode[1,2]	0	Au, Cu[e]	2A,3B, S6

Notes: **General)** Benz. and Benz. Alc. stand for benzaldehyde and benzyl alcohol, respectively. **a)** Most water peaks show contributions from both bulk (1650 cm^{-1}) and adsorbed water (~1630 cm^{-1} at –0.3 V) making Stark tuning estimates unreliable. **b)** Cu shows a slightly higher adsorbed peak and bulk shoulder at 1695 and 1702 cm^{-1}, respectively, both within error. Pd also shows a slightly higher peak at 1696 cm^{-1}. Pt shows a lower adsorbed benzaldehyde peak at 1689, likely due to interference from the adjacent water band. **c)** The benzaldehyde ring peak positions are indistinguishable for the bulk and adsorbed species, with the 1596/1598 and 1455/1454 differences falling within experimental variation. **d)** The electrochemically formed benzyl alcohol shows an identical peak position to the bulk species. **e)** On Cu, the 1496 and 1453 peaks overlap with hydrobenzoin. Benzyl alcohol likely has a significant contribution given the H stretching modes present.

Table S2. Summary of Infrared Peak Assignments Continued

Peak Position /cm^{-1}	Peak Assignment	Stark Rate cm^{-1}/V	Surfaces Present	Figures Present
3105	Ketyl Radical Intermediate[a]	0	Cu	3C, S10B
1673	Ketyl Radical Intermediate[a]	0	Cu	3A, 3B, S9
1482	Ketyl Radical Intermediate[a]	0	Au	2A, S6
3061	Hydroben, Ring H Stretch[2,b] (-10)	0	Cu	3C, S10B
3036	Hydroben, Ring H Stretch[2,b] (0)	0	Cu	3C, S10B
2900	Hydroben, Ring H Stretch[2,b] (-1)	0	Cu	3C, S10B
1963	Hydroben, Ring Mode[2,b] (+20)	0	Cu	3A, 3B, S9
1897	Hydroben, Ring Mode[2,b] (+17)	0	Cu	3A, 3B, S9
1807	Hydroben, Ring Mode[2,b] (-8)	0	Cu	3A, 3B, S9
1604	Hydroben, Ring Mode[2,b] (+1)	0	Cu	3A, 3B, S9
1496	Hydroben, Ring Mode[2,b] (+1)	0	Cu	3A, 3B, S10A
1455	Hydroben, Ring Mode[2,b] (+2)	0	Cu	3A, 3B, S10A
1191	Hydroben, Ring Mode[2,b] (+3)	0	Cu	3A, 3B
1080	Hydroben, Ring Mode[2,b] (-3)	0	Cu	3A, 3B
1022	Hydroben, Ring Mode[2,b] (-11)	0	Cu	3A, 3B
1328	Hydroben Rearrangement Product	0	Cu	3A, 3B
1344	Hydroben Rearrangement Product	0	Cu	3A, 3B
1299	Hydroben Rearrangement Product	0	Cu	3A, 3B
1258	Hydroben Rearrangement Product	0	Cu	3A, 3B
1277	Hydroben Rearrangement Product	0	Cu	3A, 3B
1220	Hydroben Rearrangement Product	0	Cu	3A, 3B

Notes: **General)** Hydroben stands for hydrobenzoin. **a)** The assigned 3105 and 1673 bands are not detectable on Au. The 1673 peak likely has interference from the strong bulk water peak on Au. The lack of a 3105 cm^{-1} peak may result from lower radical concentrations, as no ring H stretching peaks appear for Au either. The 1482 peak is not visible for Cu due to obscuration by the 1496 hydrobenzoin band. **b)** Hydrobenzoin was assigned based on comparison with the bulk spectra of meso-hydrobenzoin from the NIST data base.[2] The numbers in parentheses represent the difference in peak position between the hydrobenzoin on Cu and the bulk infrared spectrum.

Table S3. Summary of CO Infrared Peak Assignments

Peak Position /cm^{-1}	Peak Assignment	Stark Rate cm^{-1}/V	Surfaces Present	Figures Present
1717[a]	CO_M on Pd[4]	NA[b]	Pd	4
1825[a]	CO_H on Pd[4]	36	Pd	4, S11A
1910[a]	CO_B on Pd[4,5]	51	Pd	4, 5, S11A
2020[a]	CO_L on Pd[4,5]	45	Pd	4, 5, S11A
1778[a]	CO_B on Pt[6,7]	61	Pt	6, 7
1997[a,c]	CO_L on Pt[6,7]	32	Pt	6, 7
2044[c]	CO_L on Pt[6,7] Interacting with CO	NA[c]	Pt	7B
1985[c]	CO_L on Pt Interacting with Benz	NA[c]	Pt	7B

Notes: **General)** Benz stands for benzaldehyde. CO_M, CO_H, CO_B, and CO_L stand for multibonded, hallow bonded, bridge bonded, and linearly bonded CO, respectively. **a)** The CO peaks generally show strong dependence on CO concentration and change over time during the decarbonylation of benzaldehyde. The peak positions quoted represent the highest peak position observed at -0.2 V during benzaldehyde decarbonylation, see Figures 4 and 6. **b)** The CO_M peak on Pd were not discernable at higher CO coverages, preventing estimation of Stark tuning rates. **c)** The introduction of CO to the benzaldehyde saturated surface results in the appearance of new peaks, which we have assigned to CO interacting mainly with itself and CO interacting predominantly with benzaldehyde. The original peak, assigned to a convolution of interactions, also shifts slightly. See the main text for more details and alternate assignments. Potential dependent measurements were not collected after CO introduction.

Select Spectroscopic References

1. R. Zwarich, J. Smolarek and L. Goodman, *J. Mol. Spectrosc.*, 1971, **38**, 336–357.
2. NIST Spectrometry Data Center, in *NIST Chemistry WebBook, NIST Standard Reference Database Number 69*, eds. P. J. Linstrom and W. G. Mallard, National Institute of Science and Technology, Gaithersburg, MD.
3. C. Keresszegi, D. Ferri, T. Mallat and A. Baiker, *J. Phys. Chem. B*, 2005, **109**, 958–967.
4. H. Miyake, T. Okada, G. Samjeske and M. Osawa, *Phys. Chem. Chem. Phys.*, 2008, **10**, 3607–3608.
5. Y. G. Yan, Q. X. Li, S. J. Huo, M. Ma, W. Bin Cai and M. Osawa, *J. Phys. Chem. B*, 2005, **109**, 7900–7906.
6. G. A. Planes, E. Moran, J. L. Rodriguez, C. Barbero and E. Pastor, *Langmuir*, 2003, **19**, 8899–8906.
7. L. W. H. Leung and M. J. Weaver, *Langmuir*, 1990, **6**, 323–333.

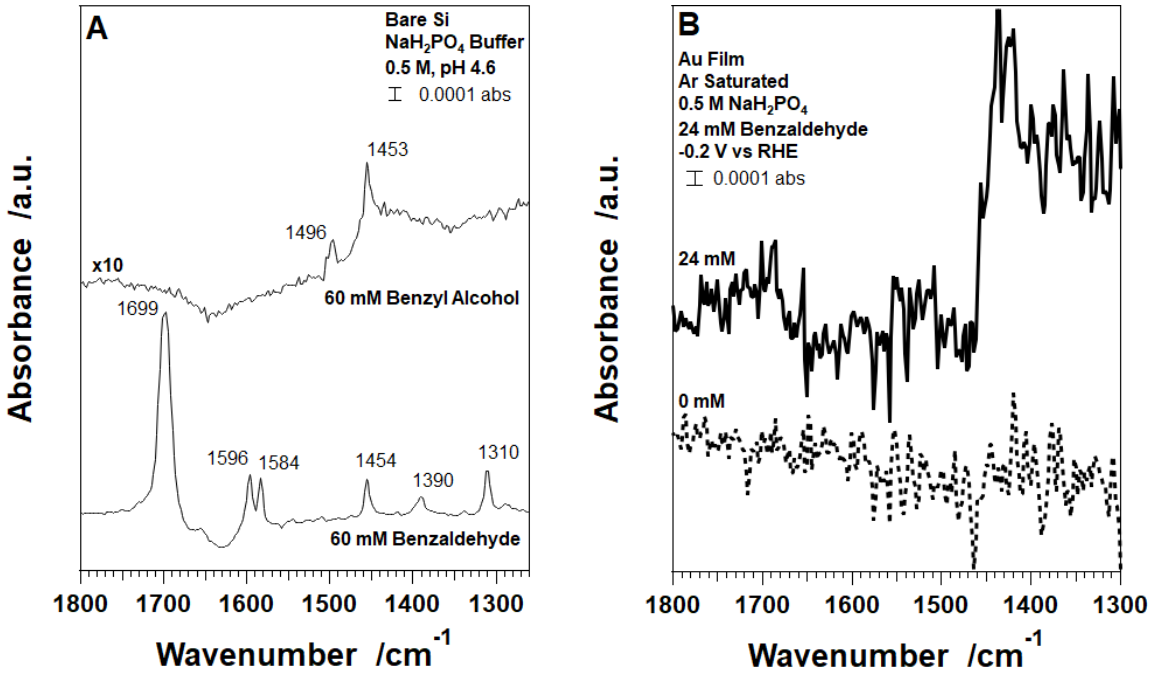

Figure S5. (A) Bulk spectra collected for benzaldehyde and benzyl alcohol on bare Si. **(B)** Spectra for benzaldehyde adsorption on Au under S-polarized light. All spectra were collected with 64 co-averaged scans and 128 background scans. Backgrounds were collected in pure phosphate buffer.

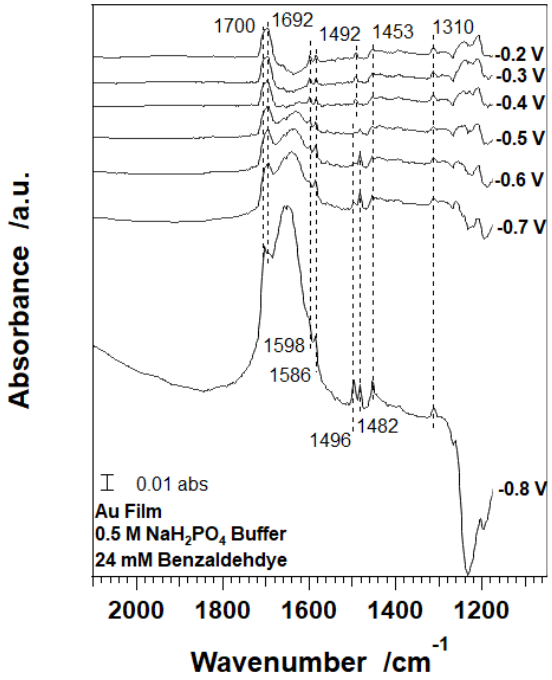

Figure S6. ATR-SEIRAS spectra collected during downward potential steps on the Au surface. Spectra represent the final spectrum collected at each potential and were collected with 64 co-averaged scans. The background was collected at -0.2 V in benzaldehyde free buffer solution.

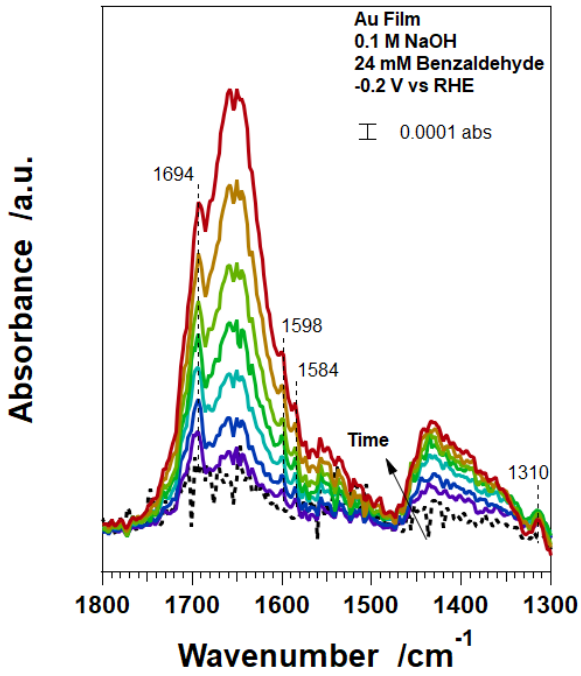

Figure S7. ATR-SEIRAS spectra for benzaldehyde introduction to Au surface in 0.1 M NaOH. The spectra were collected with 64 co-averaged scans and a background at -0.2 V in pure NaOH solution. The spectra were collected ~3 min apart with the dashed black line denoting the spectrum in NaOH.

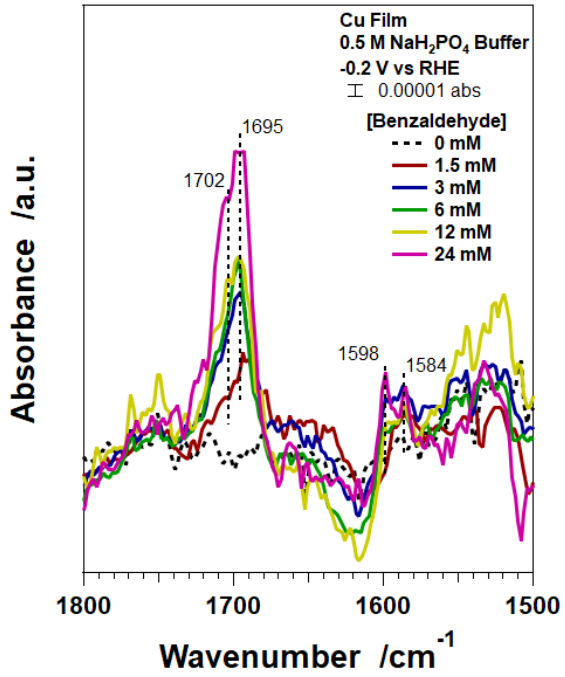

Figure S8. ATR-SEIRAS spectra for benzaldehyde adsorption on Cu at -0.2 V vs RHE. Spectra collected with 64 co-averaged scans and 128 background scans. Background collected at -0.2 V in pure buffer.

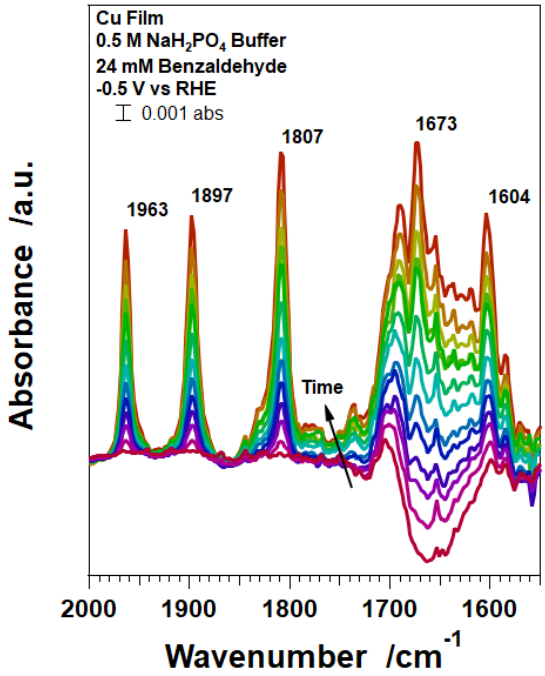

Figure S9. Time evolution spectra for the Cu surface upon stepping to -0.5 V. The spectra were collected ~6 min apart. Spectra were collected in Ar purged solution with 64 co-averaged scans. Background spectra were collected with 128 scans at -0.2 V in the absence of benzaldehyde.

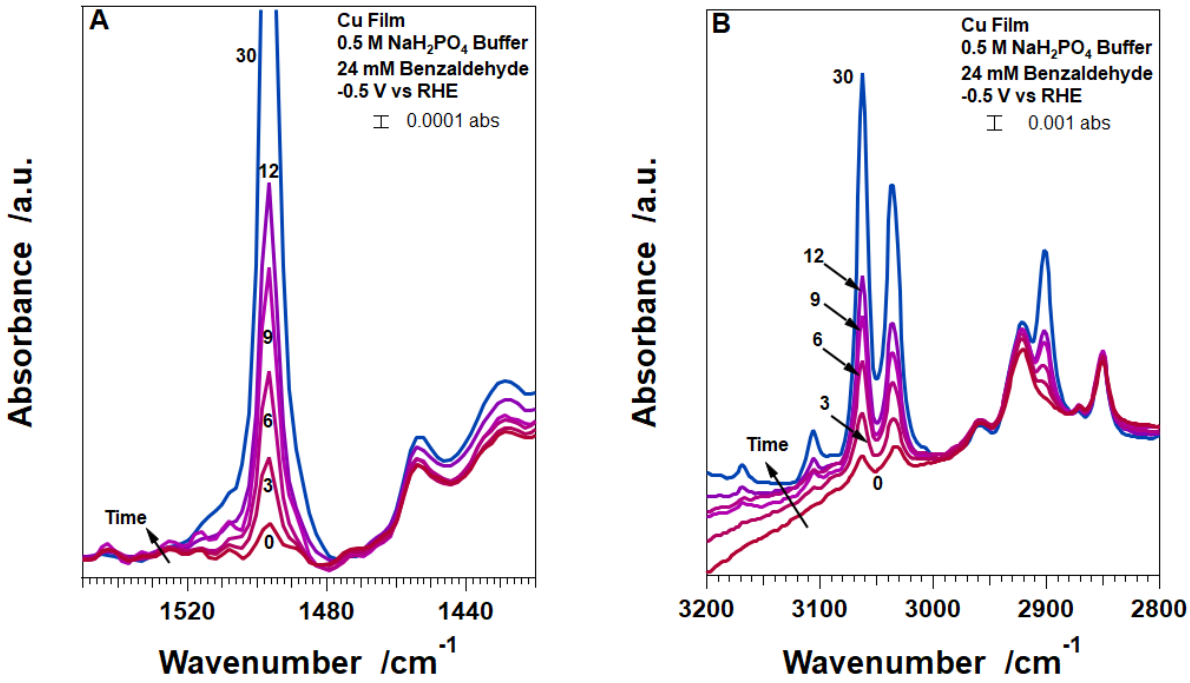

Figure S10. (A) Initial spectra for benzaldehyde reduction on Cu after reaching -0.5 V. **(B)** C-H stretching region of the same spectra in (A). Spectra were collected using 64 coadded scans, with a background collected at -0.2 V in pure buffer. The numbers refer to the approximate time (min) since reaching -0.5 V.

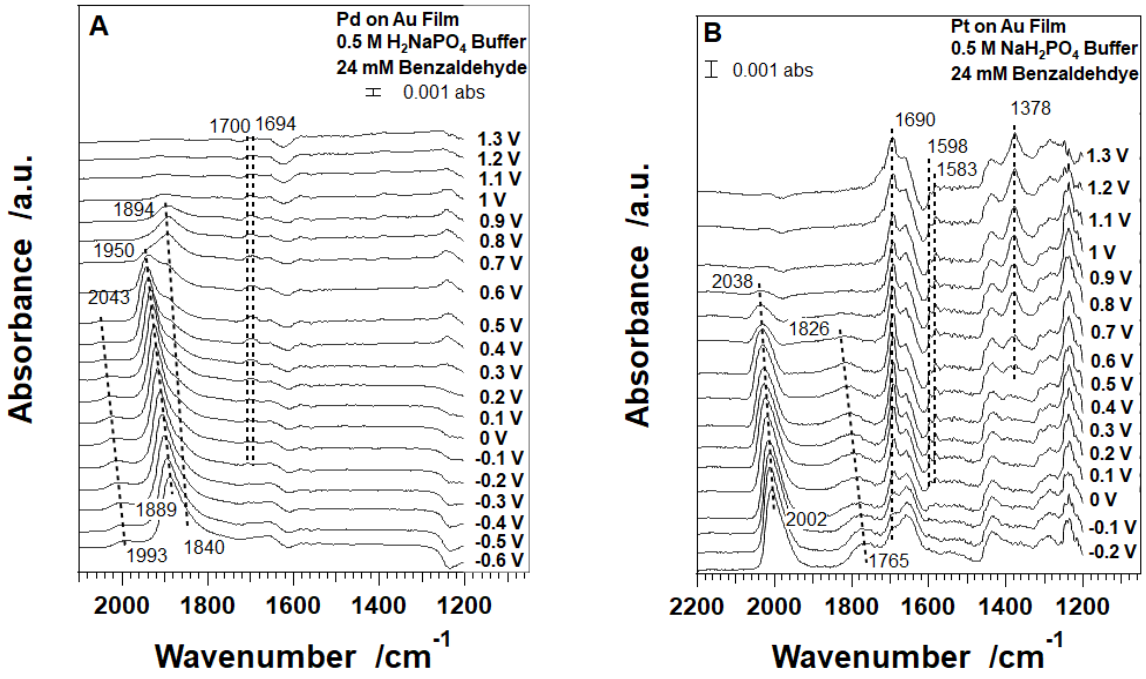

Figure S11. (A) ATR-SEIRAS collected during upward potential steps on a Pd surface in benzaldehyde solution. Background at -0.2 V. **(B)** The same set of spectra collected for a Pt surface with a background at 0 V. Both sets of spectra were collected in Ar saturated solution with 64 co-added scans and 128 background scans.